Published in final edited form as:
J Phys Chem Lett. ; 2(23): 2978–2983. doi:10.1021/jz2012319.

Water Transport through Nanotubes with Varying Interaction Strength between Tube Wall and Water

Matthew Melillo[†], **Fangqiang Zhu**[‡], **Mark A. Snyder**[†], and **Jeetain Mittal**[*,†]

[†]Lehigh University, Department of Chemical Engineering, Bethlehem, PA 18015

[‡]Laboratory of Chemical Physics, NIDDK, National Institutes of Health, Bethesda, MD

Abstract

We present the results from extensive molecular dynamics simulations to study the effect of varying interaction strength, ε_{NT-OW}, between the nanotube atoms and water's oxygen atom. We find the existence of a narrow transition region ($\varepsilon_{NT-OW} \approx 0.05$ - 0.075 kcal/mol) in which water occupancy within a nanotube and flux through it increases dramatically with increasing ε_{NT-OW}, with the exact location defined by nanotube diameter and length. This transition region narrows with increasing nanotube diameter to nearly a step-change in water transport from no flow to high water flux between ε_{NT-OW}= 0.05 kcal/mol to 0.055 kcal/mol for tube diameter 1.6 nm. Interestingly, this transition region (ε_{NT-OW}= 0.05 – 0.075 kcal/mol) also coincides with water contact angles close to 90° on an unrolled nanotube surface hinting at a fundamental link between nanotube wetting characteristics and water transport through it. Finally, we find that the observed water flux is proportional to the average water occupancy divided by the average residence time within the nanotube, with a proportionality constant found to be 0.36, independent of the nanotube diameter and length.

Keywords

nanoscale transport; wetting; hydrophobicity; nanochannels

Fluid transport through carbon nanotubes (CNTs) have been the topic of much interest recently as a greater understanding of the flow phenomenon has emerged.[1–3] They have many potential applications that cover a broad range from drug delivery and cancer therapy to nanoelectronics, gas storage and membrane separation devices.[4] The applications utilizing water transport through CNTs such as design of CNT-based desalination membranes[5–8] are of particular interest due to the fast water transport predicted by molecular dynamics (MD) simulations[9] and later observed in experiments.[10,11] Specifically, Majumder *et. al*. have shown experimentally that water flows through multi-walled CNTs at a rate that is four to five orders of magnitude faster than predicted by macroscopic hydrodynamics.[10] These flow enhancements are believed to be due to the more ordered and stronger hydrogen bonds between water molecules confined inside a nanotube than in bulk water that leads to concerted and rapid motion along the tube axis.[9] Additionally, the weak interaction between

[*]To whom correspondence should be addressed: jeetain@lehigh.edu.

water and hydrophobic walls of CNTs results in a smooth nanotube surface with minimal to zero friction.[12] The nature and magnitude of flow through small diameter CNTs is also comparable to that found in naturally occurring biological channels.[13] Therefore, gaining a more fundamental understanding of the flow mechanism through CNTs can also lead to deeper insight to the function of biological water channels.

The synthesis of individual or membrane-incorporated CNTs of a specific diameter and chirality is challenging due to lack of control over nanotube growth.[14] Also, CNT functionalization is largely limited to only the tube ends due to sp^2 hybridization of carbon along the inert tube surface, though novel ways have been proposed to overcome this limitation.[15,16] In scaling up technologies utilizing nanotubes (NTs) for specific purposes, the discovery of other materials with which NTs are easier to synthesize than carbon but possess a greater capacity for functionalization than carbon is desirable.[17,18] However, it is not clear how water transport properties will be affected. Synthesis of Boron-nitride nanotubes (BNNTs) provide some insight in this regard and have been found to have similar or better water conduction properties than CNTs.[19,20] MD simulations have shown that BNNTs of the (5,5) armchair arrangement can conduct water, while CNTs of the same size do not,[19] indicating that a difference in physical characteristics between carbon and the boron-nitride material, in this case favorable interactions with water, can be the key factor permitting water flux to occur.

In MD simulations, the difference in physical properties is usually accounted for by changing the Lennard-Jones (LJ) potential parameters - the well-depth ε and the characteristic distance σ. Boron, nitrogen, and carbon all have different LJ parameters that will dictate their interaction with water. Of course, in several cases such as Boron Nitride nanotubes there will be additional contribution from partial charges, but in the present study we solely focus on the effect of LJ interactions between NT atoms and water. In one previous study, the effect of varying partial charges on water flow through peptide backbone based nanoscopic channels was studied.[21] As we discuss later, the results found in our study are quite comparable to these findings. These parameter values for a given element are also not precisely determined and vary based on which force field is utilized in MD simulations.[22] It has been shown previously that a small variation in these parameters can cause dramatic shifts in the behavior of water in CNTs. Hummer *et. al.* observed two distinct states in which a CNT was either completely empty or completely filled with water for ε_{NT-OW} = 0.065 kcal/mol, but only a single state with a completely filled CNT existed for ε_{NT-OW} = 0.114 kcal/mol.[9] This intriguing behavior motivates this current study aimed at determining how critical a role the LJ potential well depth, ε_{NT-OW}, between the NT atoms (carbon, boron-nitride or any other element) and water's oxygen plays in influencing the flux of water through NTs. Previous work by Hummer and co-workers focused on occupancy levels and filling/emptying kinetics as a function of ε_{NT-OW} for a small diameter (6,6) NT, but did not directly calculate water flux or study larger diameter tubes.[23]

In this paper, we study water transport through cylindrical nanotubes (atoms arranged in a honeycomb lattice in an armchair arrangement) made up of different materials by systematically varying ε_{NT-OW} over a wide range. The first question that we want to address is if increasing the hydrophilicity of a nanotube surface will always result in increased water

transport through the NT. One can imagine that a continued increase in nanotube-water interaction strength will also increase residence time of molecules, in addition to increasing water occupancy. This can conceivably result in decreased water transport through hydrophilic NTs. Secondly, we want to elucidate possible analogies between transport behavior within NTs and macroscopic wetting of the NT wall. In the end, we would like to identify simple design parameters linking flow properties within specific nanotubes with water occupancy and residence time.

Through these investigations, we hope to identify a range of ε_{NT-OW} values that provide the optimum water occupancy and flux and thereby, provide design insight to guide future material selection for specific applications such as drug delivery.[24,25]

Our study focuses on understanding the sensitivity of water flow to changes in physical properties of the NT material, and thus, we use the NT atoms to represent a range of materials having different interaction strengths with water. Specifically, we simulate ε_{NT-OW} for a range of values from 0.02 kcal/mol, highly hydrophobic NTs, up to 0.20 kcal/mol, strongly hydrophilic NTs. The standard LJ potential form is used and the resulting potential functions are shown in the supplementary information (SI Fig. S1). We use TIP3P model of water for which cross-interactions between water's hydrogen atom and NT atoms are zero. For simplicity, all of the NT atoms are arranged in a honeycomb lattice as found in the case of CNTs. We arrange 12 hexagonally packed CNTs in a 3×4 membrane that allows us to accumulate 12 times more data than a single NT simulation (see Figure 1A). The nanotubes are allowed to move during the simulation, and we find that the membrane structure is maintained during the whole simulation. Here, we consider NTs of armchair types (6,6), (7,7), (8,8), (9,9), and (12,12), all of length 1.34 nm, to study diameter dependence of our results. We also consider 5.6 nm long (6,6) armchair NTs to study possible effects of NT length on the observed behavior. All of the simulations are performed using the molecular simulation package NAMD.[26] Shorter NTs are simulated for 15.2 ns and longer NTs are simulated for 30.4 ns with the first 200 ps and 400 ps, respectively, discarded as equilibration and the remaining trajectory used for all subsequent analysis. In addition, we simulate low ε_{NT-OW} values (0.04 - 0.06 kcal/mol) for (12,12) tubes for 100 ns to accommodate relatively slow filling kinetics. We also study the wetting behavior of a water droplet on a flat unrolled nanotube surface as shown in Figure 1B.

All simulations utilize periodic boundary conditions in all directions. For NT simulations, temperature and pressure are maintained at 300 K and 1 atm, respectively. The water droplet simulations are performed in an NVT ensemble at 300 K. We use PME method for electrostatic interactions. We have used Langevin thermostat with a damping coefficient of 0.5 ps^{-1} to maintain constant temperature and Langevin piston Nose-Hoover method that allows all dimensions of the periodic cell to fluctuate independently to control pressure.[27] We use 12 Å cut-off distance for pair interactions with a smoothing function applied at 9 Å distance and neighbor list radii 14 Å with a rebuilding frequency of 10 steps.

In an effort to elucidate the relation between water flow and nanotube properties, we first study how changes in ε_{NT-OW} affect the water occupancy levels (number of water molecules contained in the nanotube) in different diameters NTs. Previously, Hummer *et al*. showed

for a small diameter (0.8 nm) NT, capable of only accommodating a single-file chain of water, that an increase in ε_{NT-OW} increases the probability of observing the filled state.[9] The filled state in that case, however, was identified by a narrow occupancy level (N = 5 or 6). In Figure 2A-C, we show the probability P(N) of finding N number of water molecules inside a nanotube for several ε_{NT-OW} values. The panels A, B, and C correspond to 1.34 nm long (6,6), (9,9), and (12,12) NTs, respectively. It is clear from these plots that as the interaction strength ε_{NT-OW} increases for wider tubes (panels B and C), significantly more water molecules occupy the NTs. Due to this increase in water occupancy with increasing ε_{NT-OW}, a significant change in water structuring within the NT can also be expected.

Figure 2D shows the two-dimensional density profiles in radial-axial directions for (6,6), (9,9), and (12,12) NTs for ε_{NT-OW} values corresponding to panels A-C, with corresponding snapshots of water structure at higher occupancy shown in panel F. Only in the (6,6) NTs does there seem to be favorable axial locations (clearly seen for ε_{NT-OW} = 0.07 kcal/mol) for water molecules inside the NTs as observed earlier,[9] but this preference diminishes as ε_{NT-OW} or nanotube diameter increases. As expected, when the tubes are very hydrophilic (higher ε_{NT-OW}), the water molecules are pulled closer to the NT walls. In large diameter NTs, this effect is strong enough such that a second layer of water molecules is formed near the center of the NT (i.e., ε_{NT-OW}=0.20 for (9,9) and (12,12) NTs).

As shown in Figure 2E, the number of water molecules inside a nanotube, $\langle N \rangle$, increases with increasing ε_{NT-OW} over the entire range of values studied, with a precipitous change occurring only over a narrow range of interaction strengths (ε_{NT-OW} = 0.05 to 0.075 kcal/mol). Moreover, the change in $\langle N \rangle$ with ε_{NT-OW} becomes sharper with increasing NT diameter. Waghe *et. al.* observed a similar behavior in their study of the effect of different Lennard-Jones parameters on filling kinetics of different length (6,6) armchair CNTs. In that work, for longer tubes, in which 100 water molecules could occupy the CNT, the transition from empty to filled was much sharper than that for shorter tubes in which only 5 water molecules could fit inside.[23] Here, we show that this observation is not limited to the length of a narrow (6,6) CNT in which single-file water flow occurs. Rather, it also holds true for larger diameter tubes. Therefore, with increasing NT volume, due either to NT diameter or length, one can expect to see a sharpened sensitivity of nanotube filling/emptying to subtle changes in ε_{NT-OW}.

To identify if this transition region in ε_{NT-OW} for water occupancy may be related to NT surface wetting characteristics, we next investigate the behavior of a water droplet on an infinite unrolled NT surface as shown in Figure 1B. We calculate the contact angle θ of the water droplet on the surface by using a method proposed by Giovambattista *et. al.*[28] A surface with $Cos\theta$ greater than 0 is usually interpreted as hydrophilic, while $Cos\theta$ less than 0 indicates a hydrophobic surface. Figure 3A shows the Cosine of the contact angle θ as a function of ε_{NT-OW}. This data shows that the surface changes from highly hydrophobic, yielding a very high contact angle of 150° ($Cos\theta = -0.87$) for an ε_{NT-OW} value of 0.02 kcal/mol (Figure 3B bottom panel), to partially wetting at an ε_{NT-OW} value of ≈ 0.1 kcal/mol. For ε_{NT-OW} values of 0.14 kcal/mol and higher, the water droplet completely spreads out on the surface (Figure 3B top panel) and, therefore, the surface is completely wetted. Most importantly, we find that ε_{NT-OW} values in the transition region of Figure 2E

correspond to contact angles near 90°, the contact angle at which the surface transitions from wetting to non-wetting, thus revealing a fundamental connection between water occupancy inside NTs and Wettability of a NT surface.

The primary focus of this study, which has not been addressed in any previous study to our knowledge, is to understand how a change in ε_{NT-OW} will affect water transport through a NT membrane for NTs with different diameters and lengths. Here, we define water flux to be the total permeations of water molecules per nanosecond, where a permeation is defined as a water molecule entering either end of the NT and leaving from the opposite end. The water molecules that enter and leave the same side of the nanotube are not counted in total permeation. Again, the diameter of armchair NTs is changed by adjusting the chirality vector (n,n) and increases with n. We observe burst-like flow either due to liquid-vapor oscillations[29] through an emptying-filling nanotube or pulse-like conduction through a water-filled nanotube.[9]

In Figure 4, we plot water flux as a function of interaction strength between a NT atom and water's oxygen for NTs of length 1.34 nm (filled points) and NTs of length 5.60 nm (empty circles). Similar to water occupancy variations, this data shows that variations in ε_{NT-OW} have a dramatic effect on water flux over a very narrow range, from roughly 0.05 kcal/mol to 0.075 kcal/mol, leading to an off-on transition in water flow through the NTs. As discussed above, this transition region for ε_{NT-OW} values is the range in which NTs change from hydrophobic to hydrophilic as shown by contact angle measurements in Figure 3.

Upon closer inspection of Figure 4, we find that the change from no water transport to significant water flux becomes sharper with increasing NT diameter, a sharpening of the transition consistent with that which was observed for water occupancy (Figure 2E). As the tube diameter increases, water occupancy also increases. The concomitant increase in the number of water molecules that are able to interact with the NT surface leads to an enhanced response to the changes in interaction strength, and thus the flux increases more sharply than in smaller diameter NTs. Quite remarkably, inside the transition region extremely small increases in ε_{NT-OW}, on the order of 0.0025 kcal/mol, result in drastic increases in the water flux through a NT. This observation should impact future design strategies aimed at controlling water flow through nanotube based membranes by tuning simple properties such as temperature,[30] a topic that we are currently investigating. We find that any further increase in ε_{NT-OW} beyond $\approx$0.075 kcal/mol (boundary of the transition region) actually decreases the water flux, presumably due to longer residence times of water molecules within the hydrophilic environment of the nanotube. A similar change in water permeability with changing channel polarity was observed by Portella et al.[21] In that case the channel polarity was controlled by varying partial charges on channel atoms, and, therefore, significantly reduced water permeability was observed for high channel polarity presumably due to hydrogen bonding between water and channel atoms.

So far, we have shown that flux increases drastically for ε_{NT-OW} values in the transition region and subsequently decreases as interaction strength increases. In addition, the number of molecules occupying the NT continuously increases with increasing ε_{NT-OW} over the range of values we have tested. Such an inverse relation between water permeation and

water occupancy suggests that one needs to consider additional factors that can account for the observed behavior. An obvious parameter to consider is the residence time of a water molecule within the nanotube. We calculate average residence time τ based on all the water molecules that transmit through a NT averaged over time and plot it in Figure 5 as a function of ε_{NT-OW}. The measured τ values cover a range from 10 ps to 200 ps and increase with increasing ε_{NT-OW}, as expected due to enhanced water-nanotube interactions. Also, we notice that τ is only weakly dependent on nanotube diameter, an observation that may be very useful in developing theories of water flow through nanoscopic channels.

Since an increase in ε_{NT-OW} past the transition region leads to a decline in flux (Figure 4), an increase in occupancy (Figure 2E), and an increase in residence time (Figure 5), we anticipate that both $\langle N \rangle$ and τ will be the relevant parameters for defining water transport through nanotube based membranes, and a combination of the two may be able to explain the observed flow with changing NT diameter and length. The simplest possible functional form that one may be able to use is, flux $\propto \langle N \rangle / \tau$ with a proportionality constant that may or may not depend on tube diameter and ε_{NT-OW}. To test this, we plot observed permeation events per unit time versus $\langle N / \tau$ in Figure 6 for all NT diameters and lengths studied. Incredibly, regardless of diameter or length, a linear relationship exists yielding a slope of 0.36.

We have shown that the interaction strength between water molecules and the wall material of a nanotube, characterized by the Lennard-Jones potential well depth, has a significant impact on the ability for water molecules to enter a nanotube and reside there for a given amount of time only for a narrow range of ε_{NT-OW} values. By varying interaction strength as a design parameter representative of various materials, we have discovered a narrow transition region of values from 0.05 to 0.075 kcal/mol in which the nanotube abruptly changes from exhibiting strongly hydrophobic characteristics with zero water flux and low water occupancy, to hydrophilic behavior with extremely high water flux and relatively high occupancy. This transition region corresponds to near 90° contact angle of a water droplet measured on a flat unrolled nanotube surface. At ε_{NT-OW} values higher than 0.075, the nanotube becomes strongly hydrophilic resulting in gradually declining flux due to even greater occupancy and higher water residence times. Larger diameter nanotubes exhibit sharper transition regions and more abrupt changes in water flux and occupancy due to the larger number of interactions between water molecules and the NT wall. Finally, regardless of length, diameter or Lennard-Jones parameters, the observed water flux is proportional to average occupancy divided by average residence time.

Supplementary Material

Refer to Web version on PubMed Central for supplementary material.

Acknowledgments

We acknowledge useful discussions with Profs. Manoj Chaudhury, Anand Jagota, Tony McHugh, and Kemal Tuzla. MM is thankful to Apratim Bhattacharya for providing a code for contact angle calculations. This study utilized the high-performance computational capabilities of the Biowulf PC / Linux cluster at the National Institutes of Health, Bethesda, MD (http://biowulf.nih.gov).

References

1. Rasaiah J, Garde S, Hummer G. Water in Nonpolar Confinement: From Nanotubes to Proteins and Beyond. Annu. Rev. Phys. Chem. 2007; 59:713–740. [PubMed: 18092942]
2. Noy A, Park H, Fornasiero F, Holt J, Grigoropoulos C, Bakajin O. Nanofluidics in carbon nanotubes. Nano Today. 2007; 2:22–29.
3. Whitby M, Quirke N. Fluid flow in carbon nanotubes and nanopipes. Nat. Nanotechnol. 2007; 2:87–94. [PubMed: 18654225]
4. Alexiadis A, Kassinos S. Molecular Simulation of Water in Carbon Nanotubes. Chem. Rev. 2008; 108:5014–5034. [PubMed: 18980342]
5. Kalra A, Garde S, Hummer G. Osmotic water transport through carbon nanotube membranes. Proc. Natl. Acad. Sci. USA. 2003; 100:10175–10180. [PubMed: 12878724]
6. Corry B. Designing carbon nanotube membranes for efficient water desalination. J. Phys. Chem. B. 2008; 112:1427–1434. [PubMed: 18163610]
7. Fornasiero F, Park H, Holt J, Stadermann M, Grigoropoulos C, Noy A, Bakajin O. Ion exclusion by sub-2-nm carbon nanotube pores. Proc. Natl. Acad. Sci. USA. 2008; 105:17250. [PubMed: 18539773]
8. Yu M, Funke H, Falconer J. Gated Ion Transport through Dense Carbon Nanotube Membranes. J. Am. Chem. Soc. 2010; 132:8285–8290. [PubMed: 20504021]
9. Hummer G, Rasaiah J, Noworyta J. Water conduction through the hydrophobic channel of a carbon nanotube. Nature. 2001; 414:188–190. [PubMed: 11700553]
10. Majumder M, Chopra N, Andrews R, Hinds B. Nanoscale hydrodynamics: Enhanced flow in carbon nanotubes. Nature. 2005; 438:44–44. [PubMed: 16267546]
11. Holt J, Park H, Wang Y, Stadermann M, Artyukhin A, Grigoropoulos C, Noy A, Bakajin O. Fast mass transport through sub-2-nanometer carbon nanotubes. Science. 2006; 312:1034. [PubMed: 16709781]
12. Falk K, Sedlmeier F, Joly L, Netz RR, Bocquet L. Molecular Origin of Fast Water Transport in Carbon Nanotube Membranes: Superlubricity versus Curvature Dependent Friction. Nano Lett. 2010; 10:4067–4073. [PubMed: 20845964]
13. Zhu F, Schulten K. Water and proton conduction through carbon nanotubes as models for biological channels. Biophys. J. 2003; 85:236–244. [PubMed: 12829479]
14. Hinds B, Chopra N, Rantell T, Andrews R, Gavalas V, Bachas L. Aligned multiwalled carbon nanotube membranes. Science. 2004; 303:62. [PubMed: 14645855]
15. Majumder M, Keis K, Zhan X, Meadows C, Cole J, Hinds B. Enhanced electrostatic modulation of ionic diffusion through carbon nanotube membranes by diazonium grafting chemistry. J. Mem. Sci. 2008; 316:89–96.
16. Lee K, Li L, Dai L. Asymmetric end-functionalization of multi-walled carbon nanotubes. J. Am. Chem. Soc. 2005; 127:4122–4123. [PubMed: 15783165]
17. Hirsch A, Vostrowsky O. Functionalization of carbon nanotubes. Top. Curr. Chem. 2005:193–237.
18. Zhi C, Bando Y, Tang C, Huang Q, Golberg D. Boron nitride nanotubes: functionalization and composites. J. Mater. Chem. 2008; 18:3900–3908.
19. Won C, Aluru N. Water permeation through a subnanometer boron nitride nanotube. J. Am. Chem. Soc. 2007; 129:2748–2749. [PubMed: 17305343]
20. Won C, Aluru N. Structure and dynamics of water confined in a boron nitride nanotube. J. Phys. Chem. C. 2008; 112:1812–1818.
21. Portella G, de Groot B. Determinants of water permeability through nanoscopic hydrophilic channels. Biophys. J. 2009; 96:925–938. [PubMed: 19186131]
22. Werder T, Walther JH, Jaffe RL, Halicioglu T, Koumoutsakos P. On the Water-Carbon Interaction for Use in Molecular Dynamics Simulations of Graphite and Carbon Nanotubes. J. Phys. Chem. B. 2003; 107:1345–1352.
23. Waghe A, Rasaiah JC, Hummer G. Filling and emptying kinetics of carbon nanotubes in water. J. Chem. Phys. 2002; 117:10789–10795.

24. Chaban V, Prezhdo O. Water Boiling Inside Carbon Nanotubes: Towards Efficient Drug Release. ACS nano. 2011; 5:5647. [PubMed: 21648482]

25. Chaban V, Savchenko T, Kovalenko S, Prezhdo O. Heat-Driven Release of a Drug Molecule from Carbon Nanotubes: A Molecular Dynamics Study. J. Phys. Chem. B. 2010; 114:13481. [PubMed: 20831145]

26. Phillips J, Braun R, Wang W, Gumbart J, Tajkhorshid E, Villa E, Chipot C, Skeel R, Kale L, Schulten K. Scalable molecular dynamics with NAMD. J. Comput. Chem. 2005; 26:1781. [PubMed: 16222654]

27. Feller S, Zhang Y, Pastor R, Brooks B. Constant pressure molecular dynamics simulation: the Langevin piston method. J. Chem. Phys. 1995; 103:4613.

28. Giovambattista N, Debenedetti P, Rossky P. Effect of surface polarity on water contact angle and interfacial hydration structure. J. Phys. Chem. B. 2007; 111:9581–9587. [PubMed: 17658789]

29. Beckstein O, Sansom M. Liquid–vapor oscillations of water in hydrophobic nanopores. Proc. Nat. Acad. Sci. USA. 2003; 100:7063. [PubMed: 12740433]

30. Wang H-J, Xi X-K, Kleinhammes A, Wu Y. Temperature-induced hydrophobic-hydrophilic transition observed by water adsorption. Science. 2008; 322:80–83. [PubMed: 18832642]

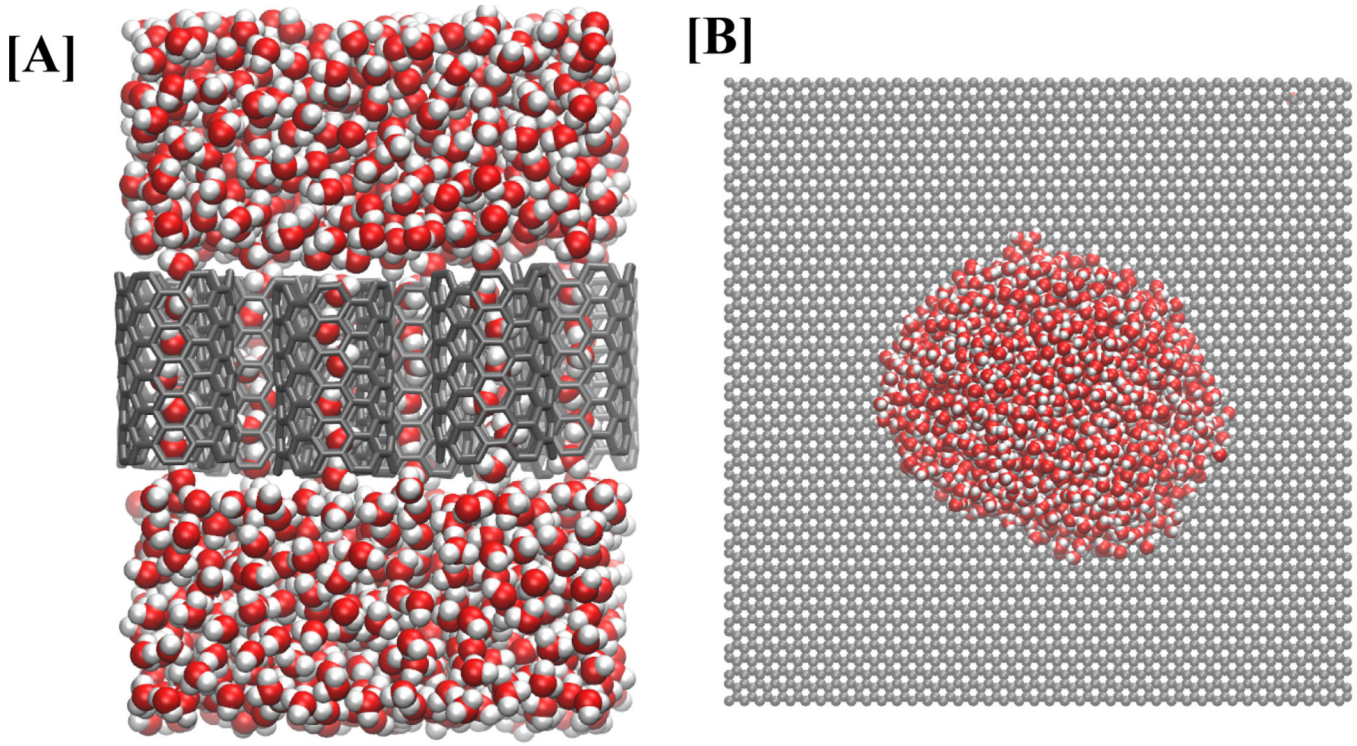

Figure 1.

System setup. (A) Side-view of nanotube membrane-water system used for most of the data presented in this paper. (B) Water droplet resting on an infinite unrolled nanotube sheet used for contact angle measurements.

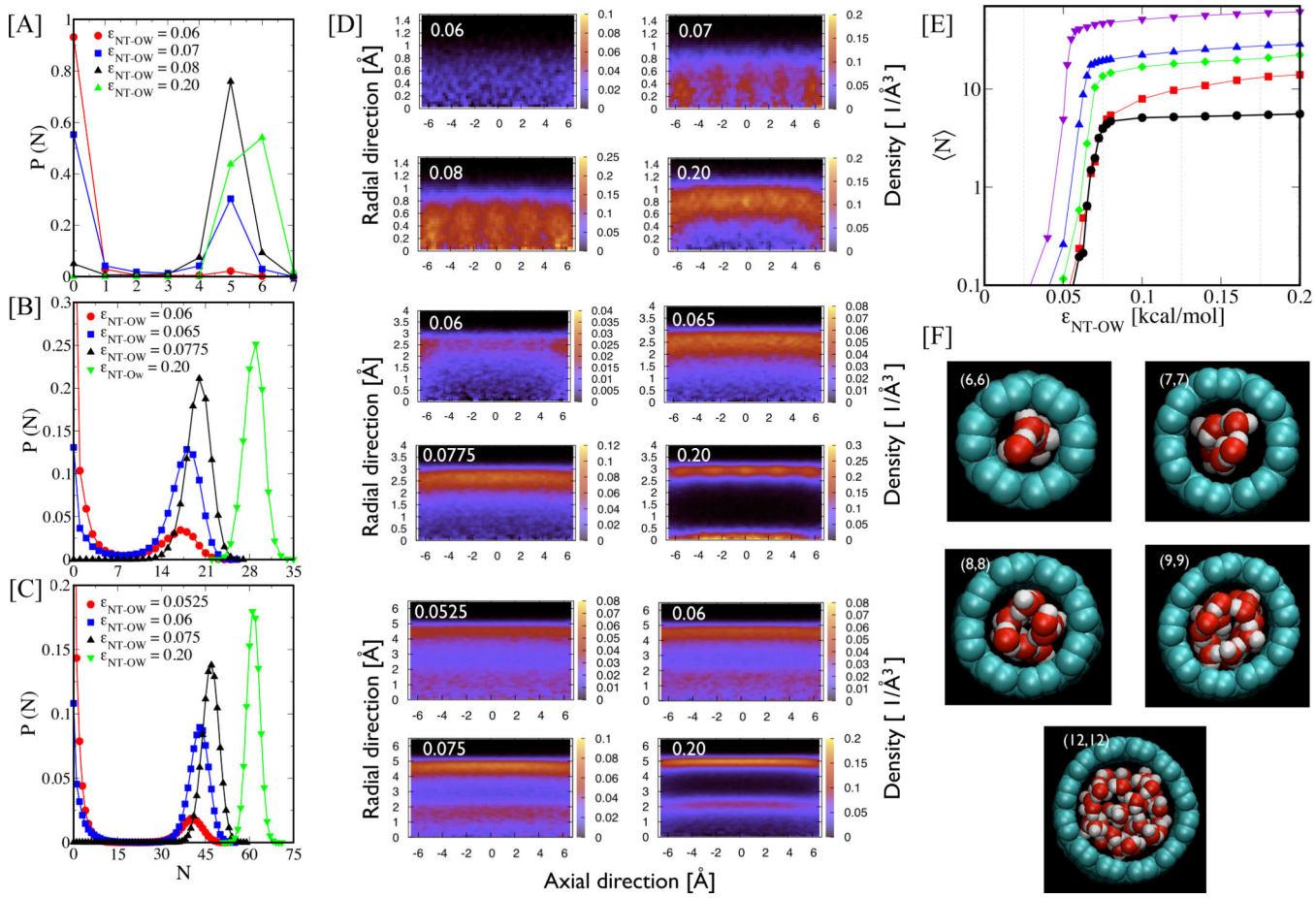

Figure 2.

Water occupancy. (A-C) Probability of a nanotube containing *N* water molecules inside it at any given time. Panels A through C are for (6,6), (9,9), and (12,12) NTs (1.34 nm long), respectively. (D) Water number density profiles as a function of radial distance away from the nanotube center and axial distance along the nanotube are shown corresponding to ε_{NT-OW} values in panels A-C. (E) Average number of water molecules occupying a nanotube $\langle N \rangle$ as a function of ε_{NT-OW} are shown for different diameter nanotubes. The curves from bottom to top correspond to (6,6), (7,7), (8,8), (9,9), and (12,12) nanotubes, respectively. (F) Representative snapshots of water molecules confined in a filled nanotube for different diameter tubes.

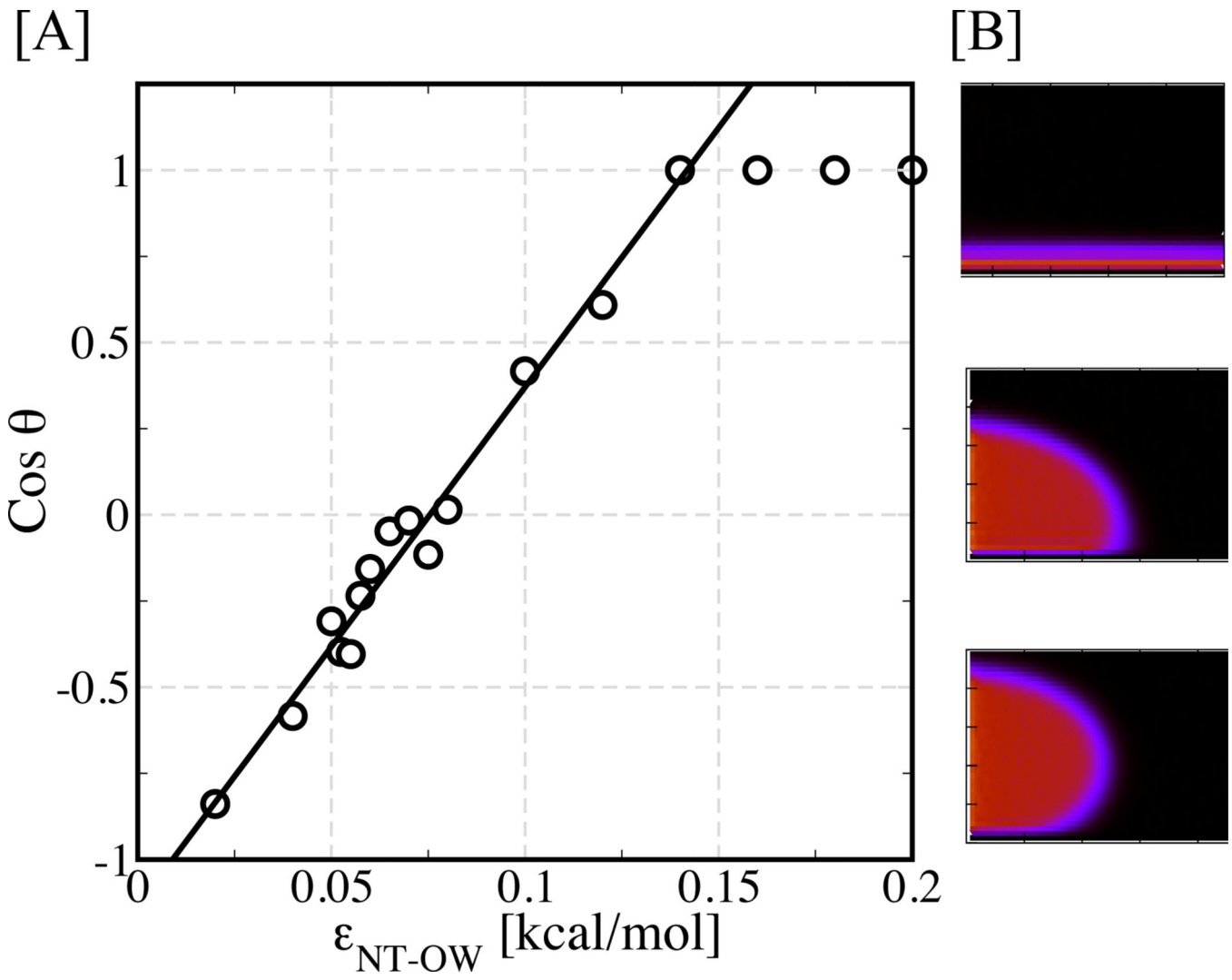

Figure 3.

Wettability of a flat surface. (A) Cosine of the contact angle of a water droplet on a graphene surface versus the nanotube material-water interaction potential strength. (B) Two-dimensional contour density plots for water droplet resting on a graphene surface with Cosine of the contact angles 1 (θ = 0°;top), 0 (θ = 90°; middle), and −0.87 (θ = 150°; bottom).

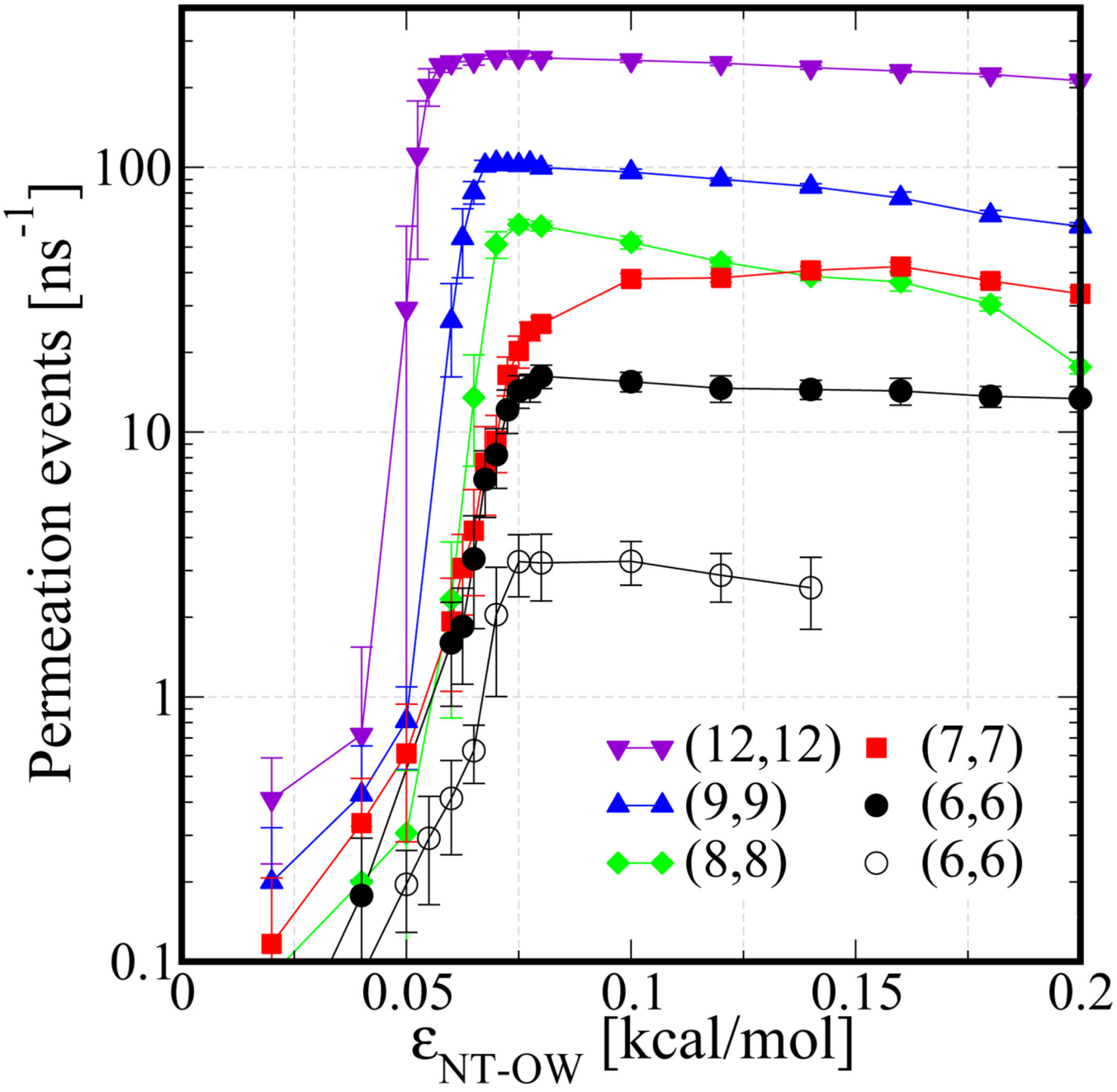

Figure 4.

Effect of nanotube-water interaction strength on water permeability. Number of water permeation events are shown as a function of nanotube-water interaction strength ε_{NT-OW} for nanotubes of different diameter and length. Diameters (from center of nanotube atoms) range from 0.82 nm in the (6,6) arrangement up to 1.66 nm in the (12,12) arrangement. The filled data points represent NTs 1.34 nm in length and the empty data points represent NTs 5.60 nm in length.

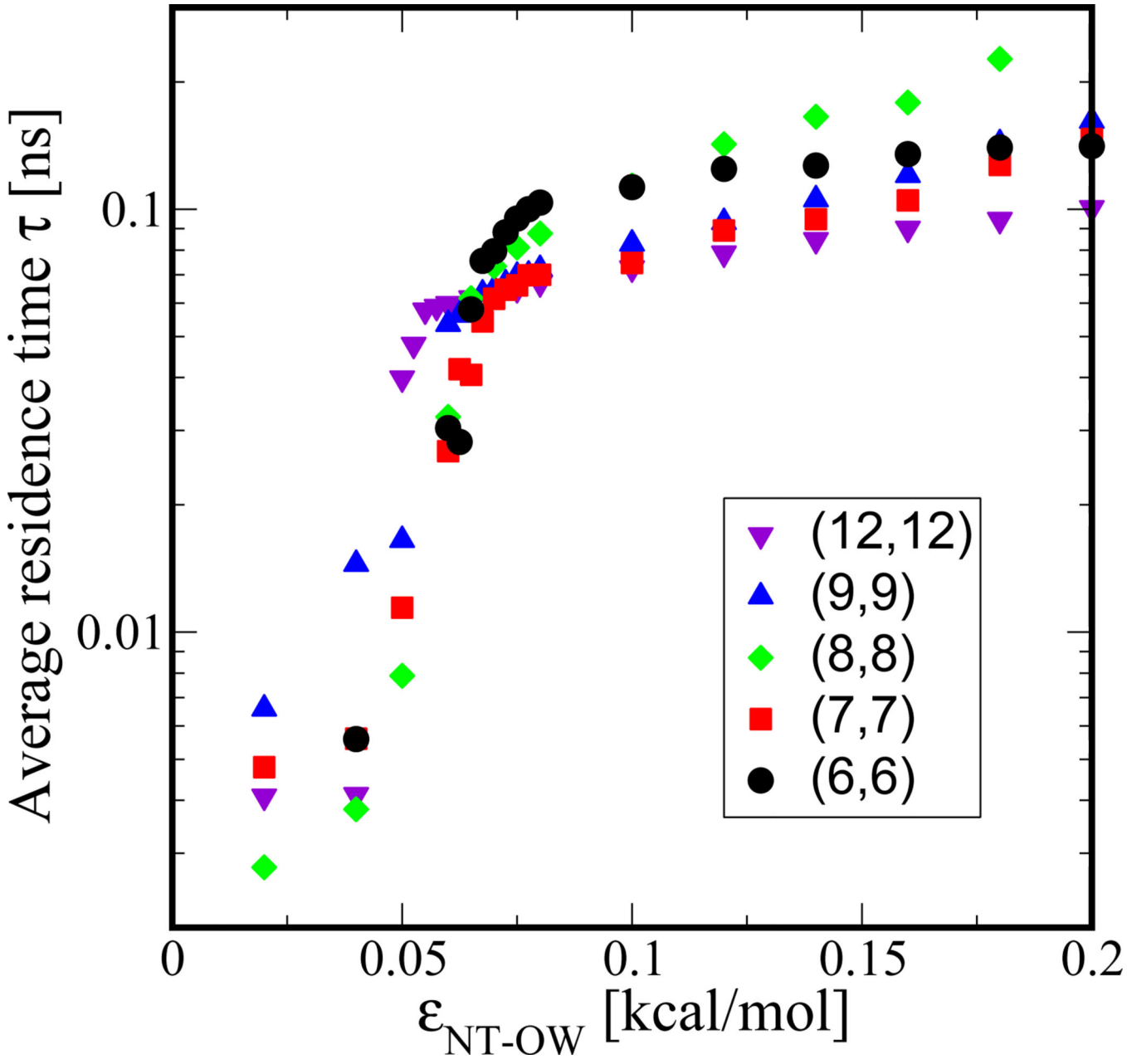

Figure 5.

Average residence time measured for water molecules that enter the nanotube from one side and leave from the other side is plotted as a function of nanotube-water interaction strength ε_{NT-OW} for different nanotube diameters as shown in the legend.

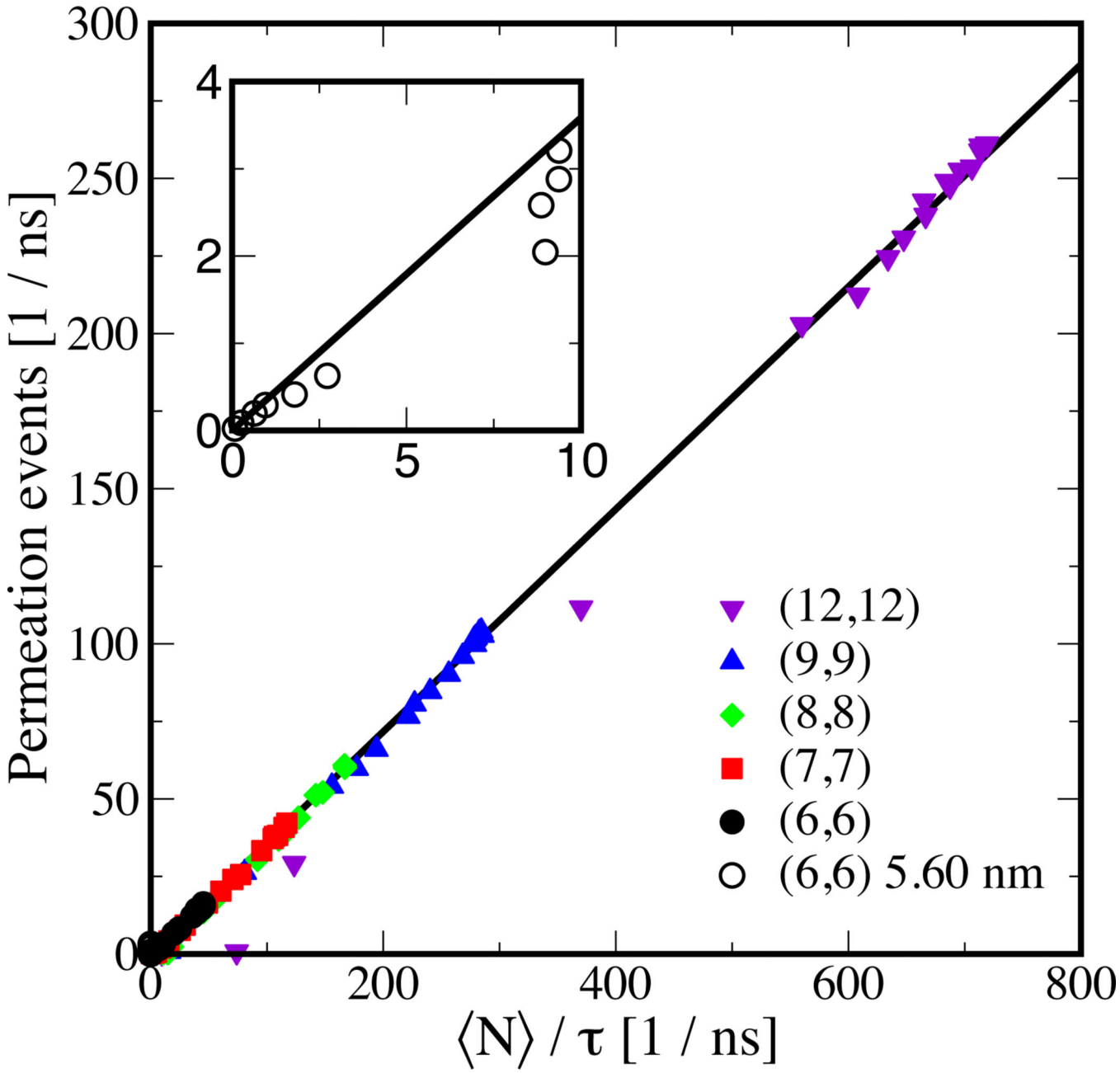

Figure 6.

Permeation events per unit time observed in molecular dynamics simulation versus average occupancy $\langle N \rangle$ divided by average residence time τ. The symbols are the simulation data and black line is a linear fit to this data. The inset shows a zoom-in view specifically to highlight longer nanotube data.